

Nucleon properties from unconventional interpolating fields

Derek B. Leinweber*

Department of Physics, The Ohio State University, 174 West 18th Avenue, Columbus, Ohio 43210-1106
(Received 31 May 1994; revised manuscript received 21 December 1994)

Interpolating fields, used to excite hadrons from the QCD vacuum in nonperturbative field-theoretic investigations of hadron properties, are explored with an emphasis on unconventional nucleon interpolators. The QCD continuum model for excited state contributions to QCD correlation functions is a central element in extracting the physics contained in these alternate correlation functions. The analysis confirms the independence of nucleon properties obtained from different interpolating fields. However, this independence comes about in a trivial manner. These results provide a resolution to the long standing debate over the optimal nucleon interpolating field to be used in QCD sum rule analyses.

PACS number(s): 12.38.Gc, 11.55.Hx, 12.38.Lg, 12.40.Yx

I. INTRODUCTION

One of the instrumental operators of nonperturbative field-theoretic investigations of hadron structure is the hadron interpolating field. This operator is used to excite a hadron of specified quantum numbers from the QCD vacuum. It has long been established that there are two independent interpolating fields with no derivatives having the quantum numbers of spin 1/2 and isospin 1/2. Both are expected to excite the ground state nucleon from the vacuum. Various linear combinations of these interpolators are used in nonperturbative approaches to QCD. What distinguishes the different approaches is the manner in which the propagation of quarks in the QCD vacuum is determined.

Numerical simulations of the theory via lattice regularization is the only method for probing deep into the nonperturbative regime of QCD. Exploitation of the operator product expansion (OPE) in QCD sum rules (SR's) allows the near-perturbative regime of QCD to be explored. Modeling of the QCD vacuum via instanton fluctuations in the random instanton liquid model (RILM) has also produced some new insights into QCD. While there are formal field-theoretic arguments indicating nucleon properties are independent of the interpolating field, a demonstration of this in practice is an important test of these approaches to nonperturbative field theory.

Some attention has been given previously to alternate nucleon interpolators on the lattice [1,2]. In these analyses conclusions were limited as the correlation functions deteriorated too quickly for ground state properties to be determined. In a previous paper [3] it was established that the properties of the lowest-lying state may be extracted from the first few points of two-point correlation functions with the use of a pole plus QCD continuum model inspired by QCD sum rule analyses. In this

paper, these techniques are used to investigate nucleon properties obtained from correlation functions of unconventional nucleon interpolating fields. Some of these correlation functions suffer a loss of signal prior to a clear ground state domination and the QCD continuum model becomes a central element in fitting the correlation functions.

In the QCD-SR field there is a history of argument over the optimum nucleon interpolating field to be used in analyses [4–11]. This issue is recognized to be of paramount importance and remains unsettled [12]. While some advocate an interpolating field for which the leading terms of the OPE are stationary with respect to the interpolating field mixing parameter [5,6], others argue that a balance between OPE convergence¹ and QCD continuum contributions must be maintained [8–11].

Ideally, one would like to simply calculate with alternate interpolating fields and confirm that the nucleon properties remain unchanged. However, the limitations of the QCD-SR approach have prevented one from doing this in practice. Limitations include uncertainties in the values of lower dimension condensates, factorization of higher dimension operators, OPE truncation and convergence issues, uncertainties surrounding the role of direct instanton contributions to the sum rules, and uncertainties in the reliability of the continuum model for excited states. Fortunately, the lattice approach is not plagued with the same limitations and the following analysis resolves this long standing debate.

The format of this paper is as follows. Section II introduces the interpolating fields explored in this analysis, the lattice techniques used, and issues encountered

*Present address: TRIUMF, 4004 Wesbrook Mall, Vancouver, BC, V6T 2A3, Canada.

¹Here and in the following, “convergence” of the OPE simply means that the highest dimension terms considered in the OPE, with their Wilson coefficients calculated to leading order in perturbation theory, are small relative to the leading terms of the OPE.

in relating lattice and continuum (lattice spacing $a \rightarrow 0$) formalisms. Section III highlights the QCD continuum model derivation. The analysis of the correlation functions is presented in Sec. IV for each interpolating field combination. The results are compared with other approaches to QCD in Sec. V. Finally the conclusions regarding interpolating field invariance and the optimal nucleon interpolator for QCD sum rules are summarized in Sec. VI.

II. LATTICE CORRELATION FUNCTIONS

A. Interpolating fields

The commonly used interpolating field for the proton in lattice calculations has the form

$$\chi_1(x) = \epsilon^{abc} [u^{Ta}(x)C\gamma_5 d^b(x)] u^c(x). \quad (2.1)$$

Here, we follow the notation of Sakurai [13]. $C = \gamma_4\gamma_2$ is the charge conjugation matrix, a, b, c are color indices, $u(x)$ is a u -quark field, and the superscript T denotes transpose. Dirac indices have been suppressed.

In the sum rule approach, it is common to find linear combinations of this interpolating field and

$$\chi_2(x) = \epsilon^{abc} [u^{Ta}(x)C d^b(x)] \gamma_5 u^c(x), \quad (2.2)$$

which vanishes in the nonrelativistic limit. *A priori*, there is no reason to exclude such an interpolating field [4], as the quark field operators of (2.2) annihilate the light current quarks of QCD. Of course, these quarks are highly relativistic when bound in the nucleon. With the use of the Fierz relations, the combination of the above two interpolating fields with a relative minus sign may be written

$$\begin{aligned} \chi_{SR}(x) &= \epsilon^{abc} [u^{Ta}(x)C\gamma_\mu u^b(x)] \gamma_5 \gamma^\mu d^c(x) \\ &= 2(\chi_2 - \chi_1), \end{aligned} \quad (2.3)$$

giving the proton interpolating field often found in sum rule calculations [8–11]. The alternate QCD sum rule interpolating field is

$$\begin{aligned} \chi_A(x) &= \frac{1}{2}\epsilon^{abc} [u^{Ta}(x)C\sigma_{\mu\nu} u^b(x)] \sigma^{\mu\nu} \gamma_5 d^c(x) \\ &= 2(\chi_2 + \chi_1). \end{aligned} \quad (2.4)$$

$$G_2(t, \vec{p}) = \sum_{\vec{x}} e^{-i\vec{p}\cdot\vec{x}} \text{tr} \left[\Gamma_4 \mathcal{F} \left(\gamma_5 S_u \gamma_5, \gamma_5 S_u \gamma_5, \tilde{C} S_d \tilde{C}^{-1} \right) \right]. \quad (2.8)$$

The interference contributions of these two interpolating fields are

$$G_2(t, \vec{p}) = \sum_{\vec{x}} e^{-i\vec{p}\cdot\vec{x}} \text{tr} \left[-\Gamma_4 \left\{ \mathcal{F} \left(S_u \gamma_5, S_u \gamma_5, \tilde{C} S_d \tilde{C}^{-1} \right) + \mathcal{F} \left(\gamma_5 S_u, \gamma_5 S_u, \tilde{C} S_d \tilde{C}^{-1} \right) \right\} \right]. \quad (2.9)$$

C. Lattice techniques

Here we briefly summarize the lattice techniques used in the following calculations. Additional details may be found in Ref. [1]. Wilson's formulation is used for both

In this analysis we will consider both interpolating fields introduced in (2.1) and (2.2) and their interference terms such that any linear combination of these interpolating fields may be investigated.

B. Correlation functions at the quark level

Hadron masses are determined through the consideration of two-point correlation functions. Here we consider the nucleon correlator

$$G_2(t, \vec{p}) = \sum_{\vec{x}} e^{-i\vec{p}\cdot\vec{x}} \text{tr} \left[\Gamma_4 \langle 0 | T \{ \chi_N(x) \bar{\chi}_N(0) \} | 0 \rangle \right], \quad (2.5)$$

where $\chi_N(x)$ may be either (2.1) or (2.2), $\Gamma_4 = (1 + \gamma_4)/4$ projects positive parity states for $\vec{p} = 0$, and tr indicates the trace over Dirac indices.

Correlation functions at the quark level are obtained through the standard procedure of contracting out time-ordered pairs of quark field operators. For the octet baryons it is convenient to define the correlation function

$$\begin{aligned} \mathcal{F}(S_{f_1}, S_{f_2}, S_{f_3}) &= \epsilon^{abc} \epsilon^{a'b'c'} \left\{ S_{f_1}^{aa'}(x, 0) \text{tr} \left[S_{f_2}^{bb'}(x, 0) S_{f_3}^{cc'} T(x, 0) \right] \right. \\ &\quad \left. + S_{f_1}^{aa'}(x, 0) S_{f_3}^{cc'} T(x, 0) S_{f_2}^{bb'}(x, 0) \right\}, \end{aligned} \quad (2.6)$$

where $S^{aa'}(x, 0) = T \{ q^a(x), \bar{q}^{a'}(0) \}$ and f_1, f_2, f_3 are flavor labels. For the proton interpolating field χ_1 of (2.1), the two-point function may be written

$$G_2(t, \vec{p}) = \sum_{\vec{x}} e^{-i\vec{p}\cdot\vec{x}} \text{tr} \left[\Gamma_4 \mathcal{F} \left(S_u, S_u, \tilde{C} S_d \tilde{C}^{-1} \right) \right], \quad (2.7)$$

where $\tilde{C} = C\gamma_5$. Similarly the two-point function corresponding to χ_2 of (2.2) may be written in the form

the gauge and fermionic action ($r = 1$). $SU(2)$ -isospin symmetry is enforced by equating the Wilson hopping parameters $\kappa_u = \kappa_d = \kappa$. Three values of κ are selected and are denoted $\kappa_1 = 0.152$, $\kappa_2 = 0.154$, and $\kappa_3 = 0.156$. To make contact with the physical world,

the mass and interpolating field coupling strengths calculated at the three values of κ are linearly extrapolated to $\kappa_{\text{cr}} = 0.1598(2)$ where an extrapolation of the squared pion mass vanishes. Differences between linear extrapolations to $m_\pi = 0$ as opposed to the physical pion mass are small and are neglected in the following.

Twenty-eight quenched gauge configurations were generated by the Cabibbo-Marinari [14] pseudo-heat-bath method on a $24 \times 12 \times 12 \times 24$ periodic lattice at $\beta = 5.9$. Configurations were selected after 5000 thermalization sweeps from a cold start, and every 1000 sweeps thereafter [15].

Dirichlet boundary conditions are used for fermions in the time direction. Time slices are labeled from 1 to 24, with the δ -function source at $t = 4$. To minimize noise in the Green functions, the parity symmetry of the correlation functions and the equal weighting of $\{U\}$ and $\{U^*\}$ gauge configurations in the lattice action are exploited. The nucleon mass determined from χ_1 of (2.1) is used to set the lattice spacing. This estimate lies between other estimates based on the string tension or the ρ -meson mass. The lattice spacing is determined to be $a = 0.132(4)$ fm and $a^{-1} = 1.49(5)$ GeV.

Statistical uncertainties in the lattice correlation functions are estimated by a single elimination jackknife [16]. A covariance matrix fit of the pole plus QCD continuum model over a range of 7 or more time slices is likely to be unreliable for 28 gauge configurations [17]. Instead we use standard statistical error analysis in which correlations among the fit parameters are accounted for. The Gauss-Newton method is used to minimize χ^2 . Uncertainties are taken from the standard error ellipse [18] at $\chi^2 = \chi_{\text{min}}^2 + 1$.

$$\chi_1^{\text{PV}} = \chi_1^L - \frac{\alpha_s}{4\pi} [-2 \ln Q^2 a^2 + (C_1^L - C_2^L - 2C_3^L)] \chi_1^L - \frac{\alpha_s}{4\pi} 2C_3^L \chi_2^L, \quad (2.13)$$

$$\chi_2^{\text{PV}} = \chi_2^L - \frac{\alpha_s}{4\pi} [-2 \ln Q^2 a^2 + (C_1^L + C_2^L)] \chi_2^L, \quad (2.14)$$

where

$$C_1^L = 37.91, \quad C_2^L = -3.21, \quad \text{and} \quad C_3^L = -0.80, \quad (2.15)$$

for the Wilson parameter $r = 1$. The important point is that the interpolating field χ_2 does not mix with χ_1 to one-loop order. Moreover, the mixing of χ_1 with χ_2 is negligible. Hence, it is possible to identify the properties of these interpolating fields determined on the lattice with those of their continuum ($a \rightarrow 0$) counterparts to a good approximation.

The dominant contribution to the coefficient C_1^L in the above expressions is from the self-energy corrections to the quark external lines. These corrections are accounted for in the mean-field-improved approach, and the remaining renormalization Z_χ associated with composite operators is relatively small. The principle renormalization constant C_1^L has been determined in the mean-field approach [20] and is used in the following. The nucleon coupling strength λ_N is determined in absolute terms, without resorting to a ratio of the QCD continuum contributions as done in [21,22]. In particular, the renormal-

D. Operator mixing

The implementation of Wilson fermions on the lattice induces mixing between the composite nucleon interpolating fields [19] of (2.1) and (2.2), reflecting the breaking of chiral symmetry. In Ref. [19] the mixing is argued to occur between

$$\begin{aligned} O_\alpha &\equiv \epsilon^{abc} [u_R^{Ta}(x) C d_R^b(x)] u_L^c(x) \\ &= \frac{1}{4} (1 - \gamma_5) (\chi_1 - \chi_2), \end{aligned} \quad (2.10a)$$

$$\begin{aligned} O_\beta &\equiv \epsilon^{abc} [u_L^{Ta}(x) C d_L^b(x)] u_L^c(x) \\ &= -\frac{1}{4} (1 - \gamma_5) (\chi_1 + \chi_2), \end{aligned} \quad (2.10b)$$

and a third operator

$$O_\gamma \equiv \epsilon^{abc} [u^{Ta}(x) C \gamma_\rho \gamma_5 d^b(x)] \gamma_L \gamma^\rho u^c(x). \quad (2.10c)$$

Here

$$u_R = \frac{1}{2} (1 + \gamma_5) u, \quad u_L = \frac{1}{2} (1 - \gamma_5) u, \quad (2.11a)$$

$$\gamma_R = \frac{1}{2} (1 + \gamma_5), \quad \text{and} \quad \gamma_L = \frac{1}{2} (1 - \gamma_5). \quad (2.11b)$$

However, there are only two operators having isospin 1/2 and spin 1/2 and it is possible to demonstrate

$$O_\gamma = -2O_\alpha, \quad (2.12)$$

via Fierz transformations. For χ_1 and χ_2 the expressions up to one-loop order in perturbation theory relating the operator matrix elements in the Pauli-Villars (PV) and lattice (L) schemes are [19]

ization at the scale of $1/a$ is

$$\chi^{\text{continuum}} = \frac{Z_{\chi N}}{a^{9/2}} \chi^L \left(1 - \frac{3\kappa}{4\kappa_{\text{cr}}} \right)^{3/2}, \quad (2.16)$$

and $Z_{\chi N} = (1 - 0.73 \alpha_V) \simeq 0.80$ at $\beta = 5.9$. The κ dependence of this wave function renormalization is very different from the naive normalization

$$\chi^{\text{continuum}} = \frac{1}{a^{9/2}} \chi^L (2\kappa)^{3/2}, \quad (2.17)$$

and is crucial to recovering the correct mass independence of the Wilson coefficient of the identity operator.

III. QCD CONTINUUM MODEL

Here we briefly review the QCD continuum model implementation in Euclidean space as examined in detail in Ref. [3]. We start with the two-point correlation function of (2.5). At the phenomenological level, one inserts a complete set of states N^i and defines

$$\langle 0 | \chi_N(0) | N^i, p, s \rangle = \lambda_N^i u(p, s), \quad (3.1)$$

where the coupling strength λ_N^i measures the ability of the interpolating field χ_N to annihilate the i th excitation with nucleon quantum numbers. For $\vec{p} = 0$ and Euclidean time $t \rightarrow \infty$, the ground state dominates and $G_2(t) \rightarrow \lambda_N^2 e^{-M_N t}$. The spectral representation is defined by

$$G_2(t) = \int_0^\infty \rho(s) e^{-st} ds, \quad (3.2)$$

and the spectral density is

$$\rho(s) = \lambda_N^2 \delta(s - M_N) + \zeta(s), \quad (3.3)$$

where $\zeta(s)$ provides the excited state contributions.

The form of the spectral density used in the QCD continuum model is determined by the leading terms of the

OPE surviving in the limit $t \rightarrow 0$. Here, the combination of interpolators $\chi_1 \bar{\chi}_1$ is considered. The derivation of the QCD continuum model contributions to other correlation functions proceeds in an analogous fashion. In Euclidean space, $G_2(t)$ has the following OPE:

$$G_2(t) \simeq \frac{3 \times 5^2}{2^8 \pi^4} \left(\frac{1}{t^6} + \frac{28 m_q a}{25 t^5} + \frac{14 m_q^2 a^2}{25 t^4} - \frac{56 \pi^2}{75} \frac{\langle : \bar{q} q : \rangle a^3}{t^3} + \dots \right). \quad (3.4)$$

The spectral density used in the QCD continuum model is defined by equating (3.2) and (3.4). The QCD continuum model is defined through the introduction of a threshold which marks the effective onset of excited states in the spectral density. Keeping the first two terms of (3.4), the phenomenology of $G_2(t)$ is

$$G_2(t) = \lambda_1^2 e^{-M_N t} + \xi \int_{s_0}^\infty \rho(s) e^{-st} ds, \quad (3.5a)$$

$$= \lambda_1^2 e^{-M_N t} + \xi \frac{3 \times 5^2}{2^8 \pi^4} e^{-s_0 t} \times \left(\left\{ \frac{1}{t^6} + \frac{s_0}{t^5} + \frac{1}{2} \frac{s_0^2}{t^4} + \frac{1}{6} \frac{s_0^3}{t^3} + \frac{1}{24} \frac{s_0^4}{t^2} + \frac{1}{120} \frac{s_0^5}{t} \right\} + \frac{28 m_q a}{25} \left\{ \frac{1}{t^5} + \frac{s_0}{t^4} + \frac{1}{2} \frac{s_0^2}{t^3} + \frac{1}{6} \frac{s_0^3}{t^2} + \frac{1}{24} \frac{s_0^4}{t} \right\} \right). \quad (3.5b)$$

The parameter ξ governs the strength of the QCD continuum model. In the continuum limit ($a \rightarrow 0$) $\xi = 1$ but here is optimized with λ_N , M_N , and s_0 to account for enhancement of the correlator in the short-time regime reflecting lattice anisotropy. ξ is an overall QCD continuum model strength and is expected to be independent of the quark mass. With this approach, the effects of lattice anisotropy may be absorbed through a combination of a larger QCD continuum model strength ($\xi > 1$) and marginally larger threshold (s_0).

Infrared lattice artifacts are not a significant problem for this approach as the Fourier transform weight $\exp(-i\vec{p} \cdot \vec{x})$ is correct for all propagator paths including those which wrap around the lattice spatial dimensions. The ultraviolet lattice cutoff may be modeled in a manner similar to that for the QCD continuum model. However, the modeling becomes insignificant by the second time slice following the source. Instead we simply discard the source and first time slice when fitting the correlation functions.

IV. LATTICE CORRELATOR FITS

A. $\langle \chi_1 \bar{\chi}_1 \rangle$ correlation function

χ_1 is the standard nucleon interpolating field used in lattice analyses. Its overlap with the nucleon ground state is excellent. This lattice correlation function is fit with (3.5) in a four-parameter search of λ_N , M_N , s_0 , and ξ in analysis intervals from $t = 6 \rightarrow t_f$ where t_f ranges from 11 to 23. Figure 1 illustrates the lattice data and

these 13 fits at our intermediate value of quark mass. Similar results are seen for $\kappa = 0.152$ and 0.156.

The similarity of the 13 pole plus QCD continuum fits establishes that the QCD continuum model effectively accounts for excited state contaminations in the correlation functions and allows the extraction of the ground state properties from a regime as small as $t = 6 \rightarrow 11$. For an in-depth examination of this correlator see Ref. [3]. The quark mass dependence of λ_N is illustrated in Fig. 2. Table I summarizes the fit parameters for the regime $t = 6 \rightarrow 20$.

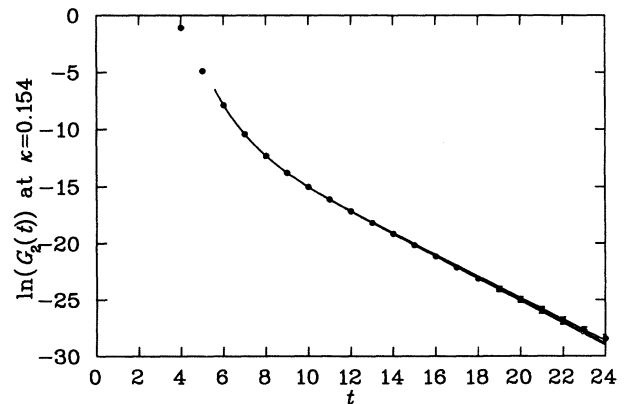


FIG. 1. The two-point correlator at $\kappa = 0.154$ for the nucleon interpolating fields $\chi_1 \bar{\chi}_1$ of (2.1). The fits for the 13 analysis intervals are illustrated. The source position is at $t_0 = 4$. Neither the source nor $t = 5$ are included in the fit.

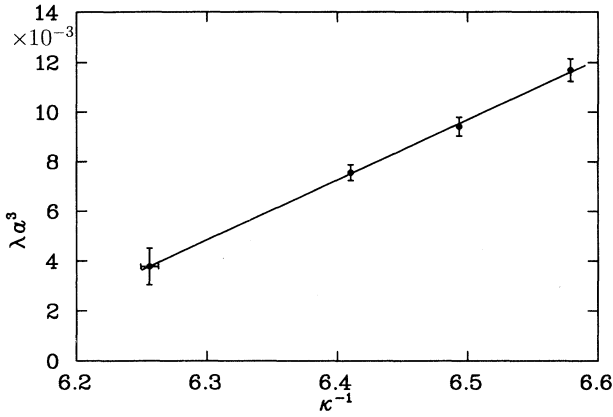


FIG. 2. The quark mass dependence of the nucleon coupling strength λ_1 corresponding to the interpolating field of (2.1).

B. $\langle \chi_2 \bar{\chi}_2 \rangle$ correlation function

Unlike QCD sum rule analyses, correlators may be determined on the lattice for any interpolating field without regard to the restrictions of OPE convergence issues or operator factorization assumptions. In constructing the QCD continuum model, only the first few terms of the OPE are required. The OPE for the interpolating fields $\chi_2 \bar{\chi}_2$ is

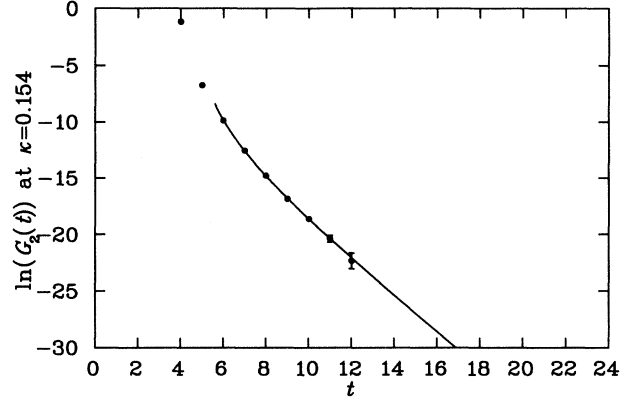


FIG. 3. Lattice correlation function for interpolating fields $\chi_2 \bar{\chi}_2$. The illustrated fit employs the QCD continuum model alone.

$$G_2(t) = \frac{3 \times 5^2}{2^8 \pi^4} \left(\frac{1}{t^6} - \frac{4}{5} \frac{m_q a}{t^5} - \frac{2}{5} \frac{m_q^2 a^2}{t^4} + \frac{8\pi^2 \langle \bar{q}q \rangle a^3}{15 t^3} + \dots \right), \quad (4.1)$$

and the QCD continuum model is derived in an analogous manner to that outlined in Sec. III. The phenomenological side of $G_2(t)$ is

$$G_2(t) = \lambda_N^2 e^{-M_N t} + \xi \frac{3 \times 5^2}{2^8 \pi^4} e^{-s_0 t} \times \left(\left\{ \frac{1}{t^6} + \frac{s_0}{t^5} + \frac{1}{2} \frac{s_0^2}{t^4} + \frac{1}{6} \frac{s_0^3}{t^3} + \frac{1}{24} \frac{s_0^4}{t^2} + \frac{1}{120} \frac{s_0^5}{t} \right\} - \frac{4 m_q a}{5} \left\{ \frac{1}{t^5} + \frac{s_0}{t^4} + \frac{1}{2} \frac{s_0^2}{t^3} + \frac{1}{6} \frac{s_0^3}{t^2} + \frac{1}{24} \frac{s_0^4}{t} \right\} \right). \quad (4.2)$$

Figure 3 illustrates the lattice correlation function and the final fit. The choice of Γ_4 in (2.5) projects out positive parity nucleon states when $\vec{p} = 0$ and therefore the correlation function must remain positive. At $t = 13$ the lattice correlation function data change sign, and indicate a loss of signal.

The fit from $t = 6 \rightarrow 12$ using a pole plus QCD continuum model leads to fit parameters where the pole lies above the continuum threshold. The position of the pole is insignificant as its removal has little effect on the χ^2/N_{DF} . Fixing the pole at the previously determined nucleon masses returns an optimum value for λ_2^2

which is negative, and once again unphysical. The fit illustrated in Fig. 3 employs the QCD continuum model alone. Hence there is no evidence of any overlap of χ_2 with the ground state nucleon in this correlation function. While the results illustrated here are for our intermediate value of quark mass considered on the lattice, similar results are seen for the lighter and heavier quark masses. The fit parameters are summarized in Table II. The QCD continuum threshold is not too different from that for $\chi_1 \bar{\chi}_1$.

Figure 4 illustrates the quark mass dependence of ξ . As anticipated, ξ is independent of m_q . This quark mass

TABLE I. $\langle \chi_1 \bar{\chi}_1 \rangle$: Four-parameter search for the pole plus QCD continuum model.

Parameter	$\kappa_1 = 0.152$	$\kappa_2 = 0.154$	$\kappa_3 = 0.156$	$\kappa_{\text{cr}} = 0.1598(2)$
$M_N a$	1.109(8)	0.983(8)	0.858(8)	0.628(17) ^a
$\lambda_1 a^3 (\times 10^{-2})$	1.17(5)	0.94(4)	0.75(3)	0.38(7)
$s_0 a$	1.68(3)	1.58(3)	1.49(4)	1.32(7)
ξ	6.83(10)	6.74(9)	6.62(9)	6.42(19)
ξ from OPE fit	5.3(1)	5.6(1)	5.8(1)	

^aThe physical proton mass sets the lattice spacing $a = 0.132(4)$ fm.

TABLE II. $\langle \chi_2 \bar{\chi}_2 \rangle$: Two-parameter search for the pure QCD continuum model.

Parameter	$\kappa_1 = 0.152$	$\kappa_2 = 0.154$	$\kappa_3 = 0.156$	$\kappa_{\text{cr}} = 0.1598(2)$
$s_0 a$	1.58(2)	1.48(2)	1.40(2)	1.23(5)
ξ	1.55(4)	1.55(4)	1.56(4)	1.56(8)
ξ from OPE fit	1.36(6)	1.34(6)	1.35(6)	

independence confirms the negative sign of the m_q correction appearing in the OPE for $\chi_2 \bar{\chi}_2$ and the use of mean-field-improved operators. It also confirms the perturbative role of the quark mass operator. While the heaviest current quark mass used in this investigation is similar to that of the strange quark, it is still light on the scale set by the nucleon mass.

It is also interesting to note that ξ is much closer to 1 than for the correlators of $\chi_1 \bar{\chi}_1$. That this might be the case is eluded to by the opposite signs of the leading terms of the OPE in (4.1), providing the possibility of cancellations in the short-time perturbative regime of the correlation function.

C. $\langle \chi_1 \bar{\chi}_2 + \chi_2 \bar{\chi}_1 \rangle$ correlation function

Since the square of λ_2 is small, one might be able to recover a signal for the overlap of the nucleon ground state and χ_2 by considering the correlation function for $\chi_1 \bar{\chi}_2$. Figure 5 illustrates a three-parameter fit from $t = 6 \rightarrow 12$ using the pole plus QCD continuum model derived from the OPE for $\frac{1}{2}(\chi_1 \bar{\chi}_2 + \chi_2 \bar{\chi}_1)$:

$$G_2(t) = \frac{3 \times 5}{2^8 \pi^4} \left(\frac{1}{t^6} - \frac{4}{5} \frac{m_q a}{t^5} - \frac{2}{5} \frac{m_q^2 a^2}{t^4} + \frac{8\pi^2}{15} \frac{\langle \bar{q}q \rangle a^3}{t^3} + \dots \right). \quad (4.3)$$

In this fit, the nucleon ground state pole position has been fixed at the previously determined nucleon masses. The fit parameters are summarized in Table III. While there is sufficient information in the correlation function

to determine a value for the nucleon mass, the corresponding uncertainties are large.

The leading terms of the OPE's for $\chi_2 \bar{\chi}_2$ and $\frac{1}{2}(\chi_1 \bar{\chi}_2 + \chi_2 \bar{\chi}_1)$ given in (4.1) and (4.3) are equivalent up to a normalization factor of 5. Since the continuum model is constructed to accommodate these leading terms, one expects the QCD continuum model parameters s_0 and ξ for these two correlators to be similar. A comparison of Tables II and III indicates that this is indeed the case.

Figure 6 illustrates the expected quark mass independence of ξ , again confirming the negative sign of the m_q correction appearing in the OPE for $\frac{1}{2}(\chi_1 \bar{\chi}_2 + \chi_2 \bar{\chi}_1)$ and the use of mean-field-improved operators. Similarly $\xi \sim 1$ as anticipated by the opposite signs of the leading terms of the OPE of (4.3).

The linear extrapolation of $(\lambda_1 \lambda_2)^{1/2}$ to κ_{cr} is illustrated in Fig. 7. The combination $(\lambda_1 \lambda_2)^{1/2}$ shows little sensitivity to the quark mass. This contrasts the dependence of λ_1 illustrated in Fig. 2, where λ_1 decreases as the quarks become lighter. Thus, λ_2 increases for decreasing quark mass. This reflects the fact that χ_2 vanishes in a nonrelativistic reduction. At the chiral limit $(\lambda_1 \lambda_2)^{1/2} = 0.0014(10) \text{ GeV}^3$. Systematic uncertainty in the extrapolated value of $(\lambda_1 \lambda_2)^{1/2}$ may be estimated using the quark mass dependence suggested by chiral perturbation theory [23] as in [3]. Here the systematic uncertainty in extrapolating is negligible relative to the statistical uncertainties.

With the previous result $\lambda_1 = 0.013(2) \text{ GeV}^3$, the nucleon coupling strength for χ_2 is found to be $\lambda_2 = 0.00016(22) \text{ GeV}^3$, approximately 100 times smaller than λ_1 . In short, there is only one nucleon interpolating field that has significant overlap with the nucleon ground state: namely,

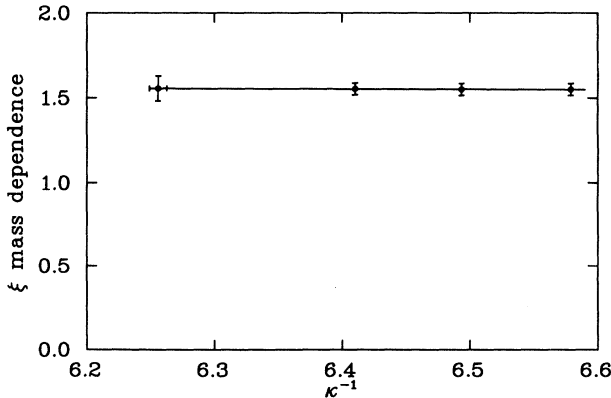


FIG. 4. The dependence of ξ on the quark mass. The displayed independence confirms the sign and magnitude for the Wilson coefficient of the m_q term in the OPE of (4.1) for $\chi_2 \bar{\chi}_2$.

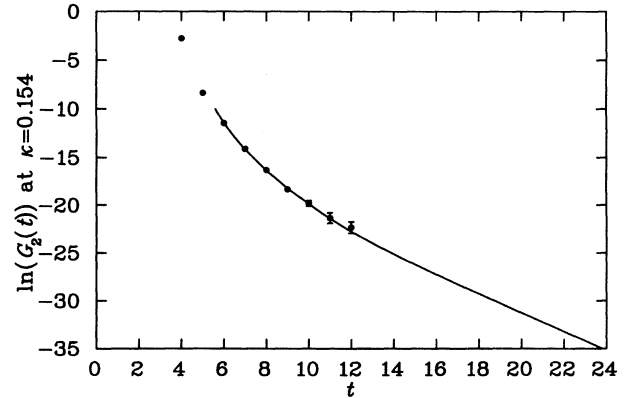


FIG. 5. Lattice correlation function for interpolating fields $\frac{1}{2}(\chi_1 \bar{\chi}_2 + \chi_2 \bar{\chi}_1)$. The nucleon mass has been fixed at the previously determined value for this fit.

TABLE III. $\frac{1}{2} \langle \chi_1 \bar{\chi}_2 + \chi_2 \bar{\chi}_1 \rangle$: Three-parameter search for the pole plus QCD continuum model. M_N has been fixed to the previously determined lattice values.

Parameter	$\kappa_1 = 0.152$	$\kappa_2 = 0.154$	$\kappa_3 = 0.156$	$\kappa_{cr} = 0.1598(2)$
$(\lambda_1 \lambda_2)^{1/2} a^3 (\times 10^{-3})$	0.50(14)	0.42(15)	0.47(14)	0.43(30)
$s_0 a$	1.55(5)	1.45(6)	1.36(7)	1.18(14)
ξ	1.57(4)	1.57(4)	1.57(4)	1.57(10)
ξ from OPE fit	1.42(4)	1.41(5)	1.42(4)	

$$\chi_1(x) = \epsilon^{abc} [u^{Ta}(x) C \gamma_5 d^b(x)] u^c(x) \quad (4.4)$$

and

$$\lambda_{SR} \simeq \lambda_A \simeq 2\lambda_1 = 0.026(4) \text{ GeV}^3, \quad (4.5)$$

$$\lambda_2 \simeq 0. \quad (4.6)$$

The results for all the considered interpolating fields are summarized in Table IV [24].

V. COMPARISON WITH OTHER CALCULATIONS

It is worth noting that the nonperturbative QCD sum rule predictions for λ_{SR} have remained quite stable over the years, despite the fact that the early calculations have a number of numerical errors in Wilson coefficients and anomalous dimensions [25]. This cannot be said for the more model-dependent predictions. It is ironic that, in some cases, the model calculations were pursued due to reservations about the reliability or validity of the QCD sum rule approach. Table V summarizes a collection of predictions taken and updated from Refs. [26] and [27].

QCD sum rule predictions of λ_2 or λ_A are more uncertain. This is largely due to a lack of rigor in the analysis of the sum rules. Often, the region of validity in Borel space is simply postulated with little regard to OPE convergence or the size of continuum model contributions. Many authors have fixed the continuum threshold to a preferred value or excitation energy rather than leaving it

as a search parameter to be optimized. The upper limit of the Borel region must be monitored as it is a function of the three required fit parameters M_N , λ_N , and s_0 and varies for different interpolating fields. The failure to monitor these issues in existing analyses is largely responsible for the apparent inconsistencies between sum rules derived from different interpolating fields.

Reference [9] is one of the few sum rule analyses where these issues are rigorously implemented. However, the interpolating field χ_2 was not considered there. The sign of the quark condensate term in (4.1) indicates that the two sum rules will be saturated by both positive and negative parity states. A careful analysis of these sum rules has not yet been attempted.

In the QCD-SR discussion of Ref. [7] it was concluded that the overlap of χ_A with the nucleon λ_A must be negligible, due to the vanishing of most of the Wilson coefficients to dimension 8. However, this conclusion need not be the case. Higher order terms of the OPE starting at dimension 9 are not zero and could easily give rise to large overlap with the nucleon as discovered here. The only conclusion that may be drawn from these sum rules is that the pole contribution is small *relative* to the QCD continuum model contribution. The pole contribution is not necessarily small in *absolute* terms.

The first five entries of Table V summarize results for λ_{SR} obtained from the consideration of two-point correlation functions, and these compare favorably. The same cannot be said for λ_A . The RILM prediction [28] is $\lambda_A = 0.040(2) \text{ GeV}^3$ and is large compared to the lattice prediction of $\lambda_A = 0.027(5) \text{ GeV}^3$. Figure 3 of Ref. [28] displays significant discrepancies between a global fit

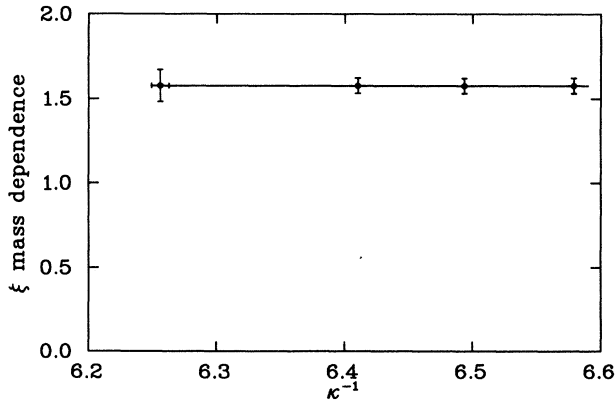


FIG. 6. The dependence of ξ on the quark mass. The displayed independence confirms the sign and magnitude for the Wilson coefficient of the m_q term in the OPE of (4.3) for $\frac{1}{2}(\chi_1 \bar{\chi}_2 + \chi_2 \bar{\chi}_1)$.

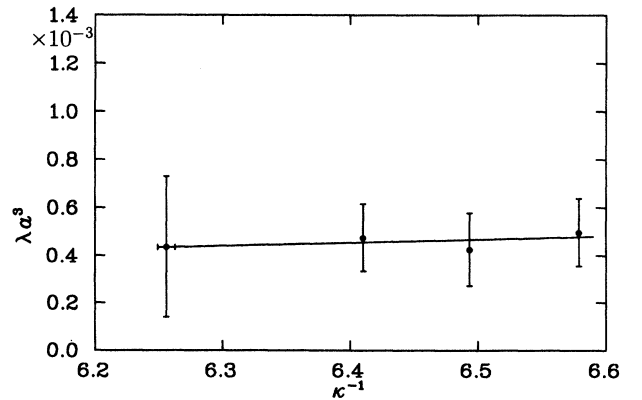


FIG. 7. Linear extrapolation of the coupling strength $(\lambda_1 \lambda_2)^{1/2}$ to κ_{cr} . The y -axis scale is one-tenth of that in Fig. 2.

TABLE IV. Summary of lattice results for the pole plus QCD continuum model.

Interpolating fields	M_N (GeV)	λ_N (GeV ³)	ξ	s_0 (GeV)
$\chi_1 = \epsilon^{abc} \left(u^a C \gamma_5 d^b \right) u^c$	0.938 ^a	0.013(2)	6.42(19)	1.98(11)
$\chi_2 = \epsilon^{abc} \left(u^a C d^b \right) \gamma_5 u^c$	Not seen	0.00016(22) ^b	1.56(7)	1.84(7)
$\frac{1}{2} (\chi_1 \bar{\chi}_2 + \chi_2 \bar{\chi}_1)$	Fixed	0.0014(10)	1.58(9)	1.76(20)
$\chi_{SR} = \epsilon^{abc} \left(u^a C \gamma_\mu u^b \right) \gamma_5 \gamma^\mu d^c$	0.96(3)	0.027(5)	4.61(14)	1.92(11)
$\chi_A = \frac{1}{2} \epsilon^{abc} \left(u^{T a} C \sigma_{\mu\nu} u^b \right) \sigma^{\mu\nu} \gamma_5 d^c$	0.91(3)	0.022(5)	3.54(10)	1.82(10)

^aDefines the lattice spacing a .

^bInferred from $\chi_1 \bar{\chi}_1$ and $\frac{1}{2} (\chi_1 \bar{\chi}_2 + \chi_2 \bar{\chi}_1)$ results.

of the six nucleon correlators considered and two of the correlators. These two correlators are both dependent on λ_A and these discrepancies are not reflected in their quoted uncertainty of ± 0.002 GeV³. Their conclusion, “What is even more important, the simple ‘nucleon pole plus continuum’ model gives a very good simultaneous description for the complete set of correlation functions,” is difficult to justify in the RILM, particularly in light of these new results.

VI. CONCLUSIONS

A. Interpolating field invariance

Ground state nucleon properties *are* independent of the interpolating field used to excite the baryon from the vacuum. This invariance is satisfied in a trivial manner. The interpolating field, which vanishes in the nonrelativistic limit,

$$\chi_2(x) = \epsilon^{abc} [u^{T a}(x) C d^b(x)] \gamma_5 u^c(x), \quad (6.1)$$

has negligible overlap with the nucleon ground state. In-

clusion of χ_2 components in interpolating fields only increases the statistical uncertainties of lattice QCD correlation functions.

B. Optimal interpolator for QCD sum rules

This analysis indicates that, to a good approximation, χ_2 excites pure QCD continuum. Since χ_2 has negligible overlap with the ground state nucleon, it is tempting to simply conclude that the optimum interpolating field is χ_1 . While this is certainly the case for lattice QCD investigations, it is not obviously the case for QCD sum rule analyses.

The optimal nucleon interpolator must involve χ_1 as this interpolator is required to maintain overlap with the ground state. The task is to determine the optimal mixing of χ_2 . The Borel-improved QCD sum rules for the generalized interpolator,

$$\chi_O = \chi_1 + \beta \chi_2, \quad (6.2)$$

are

$$\begin{aligned} & \frac{5 + 2\beta + 5\beta^2}{64} M^6 L^{-4/9} \left[1 - e^{-s_0^2/M^2} \left(\frac{s_0^4}{2M^4} + \frac{s_0^2}{M^2} + 1 \right) \right] + \frac{5 + 2\beta + 5\beta^2}{256} b M^2 L^{-4/9} \left[1 - e^{-s_0^2/M^2} \right] \\ & + \frac{7 - 2\beta - 5\beta^2}{24} a^2 L^{4/9} - \frac{13 - 2\beta - 11\beta^2}{96} \frac{m_0^2 a^2}{M^2} = \tilde{\lambda}_O^2 e^{-M_N^2/M^2} + \tilde{\lambda}_{O^*}^2 e^{-M_{N^*}^2/M^2} \end{aligned} \quad (6.3a)$$

and

TABLE V. Comparison of predictions for λ_{SR} for various approaches to QCD.

Approach	Reference	λ_{SR} ($\times 10^{-2}$ GeV ³)
Lattice (mean-field improved)	This work	2.7(5)
Lattice (conventional renormalization)	Gavela <i>et al.</i> [27]	2.4
Lattice (coordinate space)	Chu <i>et al.</i> [22]	2.2(4)
QCD sum rule	Leinweber [9]	3.1(6)
Instanton liquid	Schäfer <i>et al.</i> [28]	3.2(1)
Baryon wave functions ($x^2 \rightarrow 0$)	Brodsky <i>et al.</i> [26]	12
Quark model	Thomas and McKellar [37]	8
Bethe-Salpeter amplitude	Tomozawa [38]	2.5
MIT bag model	Donoghue and Golowich [39]	1.27
Quark model	Milosevic <i>et al.</i> [40]	2

$$\begin{aligned}
& \frac{7 - 2\beta - 5\beta^2}{16} a M^4 \left[1 - e^{-s_0^2/M^2} \left(\frac{s_0^2}{M^2} + 1 \right) \right] \\
& - \frac{3(1 - \beta^2)}{16} m_0^2 a M^2 L^{-4/9} \left[1 - e^{-s_0^2/M^2} \right] \\
& + \frac{3 + 2\beta - 5\beta^2}{2^7} a b \\
& = \tilde{\lambda}_{\mathcal{O}}^2 M_N e^{-M_N^2/M^2} - \tilde{\lambda}_{\mathcal{O}^*}^2 M_{N^*} e^{-M_{N^*}^2/M^2}, \quad (6.3b)
\end{aligned}$$

where

$$a = -(2\pi)^2 \langle \bar{q}q \rangle = 0.450 \text{ GeV}^3, \quad (6.4a)$$

$$b = (2\pi)^2 \left\langle \frac{\alpha_s}{\pi} G_{\mu\nu}^a G^{a\mu\nu} \right\rangle = 0.474 \text{ GeV}^4, \quad (6.4b)$$

$$m_0^2 = -\frac{\langle \bar{q}g\sigma Gq \rangle}{\langle \bar{q}q \rangle} = 0.65, \quad (6.4c)$$

$$L = \frac{\ln(M/\Lambda_{\text{QCD}})}{\ln(\mu/\Lambda_{\text{QCD}})}, \quad (6.4d)$$

$$\tilde{\lambda}_{\mathcal{O}} = (2\pi)^2 \lambda_{\mathcal{O}}. \quad (6.4e)$$

Here M is the Borel parameter and plays a role similar to the inverse Euclidean time of the Lattice approach. The condensate values are taken from Ref. [9] where $\mu = 0.5$ GeV and $\Lambda_{\text{QCD}} = 0.1$ GeV. The continuum model contributions are indicated on the left-hand side of the sum rules where they appear in brackets as subtractions from the terms of the OPE surviving in the limit $M \rightarrow \infty$. To aid the following discussion, both a positive parity ground state and a negative parity excited state are included on the right-hand side of the sum rules.

The first QCD SR of (6.3a) is known to have uncontrollably large perturbative corrections to the Wilson coefficient of the identity operator [29]. In leading order, these corrections are independent of β and are approximately 50%. As a result this sum rule must be discarded [30].

In the QCD-SR approach, approximations are made at both the quark level and the phenomenological level. At the quark level, the OPE is truncated and the Wilson coefficients are calculated perturbatively. This sets a lower limit for the Borel mass. At the phenomenological level, the spectral density is approximated by a pole plus the QCD continuum model. Maintaining ground state dominance on the phenomenological side of the sum rule sets an upper limit on the Borel mass. By including χ_2 components in an interpolating field, one can reduce the continuum contributions excited by χ_1 and allow a broader Borel analysis window.

One of the most difficult things to monitor in the QCD-SR approach is whether the OPE is sufficiently convergent for a particular value of Borel mass. The lattice results presented here indicate the $\chi_2\bar{\chi}_2$ correlator has the fastest converging OPE, as its overlap with the nucleon ground state is negligible. Similarly, the combination $\chi_1\bar{\chi}_1$ produces an OPE with the slowest convergence, as this correlation function is dominated by the ground state nucleon for small Borel masses.

Hence, errors made in truncating the OPE are dominated by errors in the $\chi_1\bar{\chi}_1$ component of the general

correlator. The relative error in the OPE truncation can be reduced by adding χ_2 components to the correlator. However, the χ_2 components in the OPE are simply subtracted off again by the continuum model terms. Hence the relevant error is the absolute error. For $|\beta| \lesssim 1$, this error is dominated by $\chi_1\bar{\chi}_1$ components of the correlator. As a result, OPE truncation errors are approximately independent of β . This crucial point has been neglected in previous arguments regarding the optimal nucleon interpolating field.

Since χ_2 has negligible overlap with the nucleon, the ground state contribution is also independent of β . Hence, the size of the continuum model contributions is the predominant factor in determining the optimal interpolator. Figure 8 illustrates the contributions of the continuum model terms in (6.3b) for $M = 0.938$ GeV and $s_0 = 1.4$ GeV. The following discussion is not dependent on the precise values of these parameters. The first point to be made is that contributions from the continuum model are largest for $\beta \sim -0.2$. This selection of mixing is the worst possible choice for extracting information on the ground state nucleon.

Figure 8 also indicates it is possible to have vanishing continuum model contributions at $\beta \simeq -1.5$ or $\beta = 1$. However, we are relying on the continuum model to account for strength in the correlator that does not have its origin in the ground state. Without a continuum model, one would need to include additional poles on the right-hand side of (6.3b) to account for positive and negative parity excitation strength. For $\beta < -1.5$ or $\beta > 1.0$ the correlator is negative, indicating the sum rule is saturated by a negative parity state.

Thus the optimal interpolator is $\beta \sim -1.2$ or $\beta \sim 0.8$. To discriminate between these two regimes, we turn to the higher dimension operators (HDO's) which do not contribute to the continuum model. It is these terms that provide crucial information on whether the strength in the correlator lies in the ground state or the excited states. If these terms are absent, the optimal fit of the

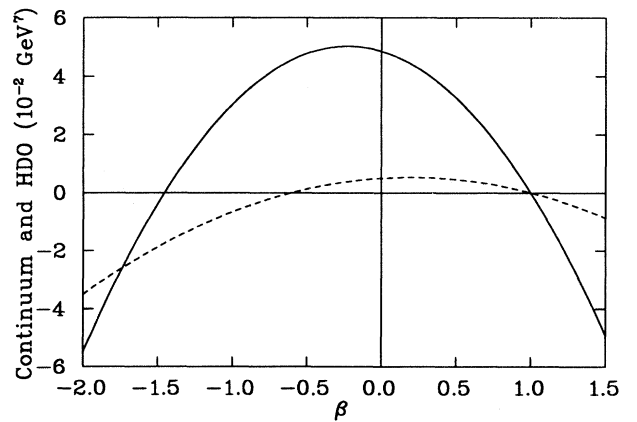


FIG. 8. Continuum model (solid curve) and higher dimension operator (HDO) (dashed curve) contributions to the Borel-improved QCD SR of (6.3b) plotted as a function of the interpolating field mixing parameter β .

correlator is obtained when $\tilde{\lambda}_O \rightarrow 0$ and $s_0 \rightarrow 0$. In this case the continuum model becomes the Laplace transform and the fit is perfect. Hence the HDO terms should be large in magnitude. A change in sign from the leading terms of the OPE will also assist in distinguishing ground state strength from excited state strength as the change in the curvature of the correlator will be more prominent.

The last term of (6.3b) is a HDO term, and its value is plotted as a function of β in Fig. 8. Once again, the regime surrounding $\beta \sim -0.2$ is undesirable. The HDO contributions are larger for $\beta \sim -1.2$ than for $\beta \sim 0.8$. In addition, the sign of the HDO contribution is opposite that of the continuum model contributions. Hence the preferred regime is $\beta \sim -1.2$. In fact, optimization of the three fit parameters M_N , $\tilde{\lambda}_O$, and s_0 , ($\tilde{\lambda}_O = 0$) of (6.3b) for $\beta = 0.6 \rightarrow 0.8$ results in fit parameters describing pure continuum with $s_0 \sim M_N$. Information to separate the ground state pole from the continuum is insufficient for $\beta = 0.6 \rightarrow 0.8$.

In summary, the lattice results indicate OPE convergence, and ground state pole contributions are approximately independent of β . Consideration of the size of continuum model contributions and the sign and magnitude of HDO operators leads to the preferred value of

$$\beta = -1.2 \pm 0.1. \quad (6.5)$$

A more precise determination of β will depend on the details of limits for continuum model contributions, HDO values, condensate values, and other parameters of the sum rules.

Hence, this analysis supports the selection of $\beta = -1$ [7–11], over $\beta = -0.2$ [4–6]. At $\beta = -0.2$, where the leading terms of the OPE are stationary with respect to β [5,6], the continuum contributions are maximal. The positive value and small magnitude of the HDO indicates that the stability of the leading terms of the OPE will not be realized as stability in the ground state mass, coupling, or in the continuum threshold.

C. Future investigations

These techniques may be used to determine the optimal interpolating field for any sum rule involving χ_1 and χ_2 components. Each sum rule will have an optimal selection for β . The overlap of spin-1/2 and spin-3/2 interpolating fields is known to yield nucleon sum rules which offer stability in the fit parameters [9] that cannot be obtained from the more common sum rules considered here. It will be interesting to discover if the historical selection of $\beta = -1$ is indeed optimal.

While it is important to establish the optimal mixing of interpolating fields for QCD-SR analyses, one should not overlook the fact that there is a range of values for β where the sum rules are expected to work. Moreover, the ground state contribution to all these sum rules is equivalent to the 1% level. In other words, the right-hand side of (6.3b) for a single pole plus continuum model is independent of β . After the first sum rule is written down, additional sum rules may be introduced with merely one

new fit parameter (s_0) per sum rule. Since direct instanton contributions to the sum rules are not independent of β [31], one has an excellent opportunity to see if direct instanton contributions really are necessary to maintain sum rule consistency [32].

Future lattice QCD investigations should aim to make a direct comparison of the OPE and lattice correlation functions. The Wilson coefficients and vacuum expectation values of normal-ordered operators could be determined directly from OPE fits to the lattice data. Such a comparison would test the validity of the OPE in the nonperturbative sector and our understanding of quantum field theory [33].

A direct comparison of lattice and continuum formalisms requires the use of an improved [34] or perfect [35] lattice action to reduce or eliminate lattice anisotropy in the short-time regime of lattice correlation functions [3,36]. Alternatively, the Wilson coefficients of the Euclidean-space correlation function may be derived via lattice perturbation theory.

An extremely fine lattice spacing is required to provide a sufficient number of lattice sites within the radius of convergence of the OPE. In the most optimistic case, the two invariant nucleon sum rules of a given interpolator could be isolated such that, to dimension 8, each correlation function would have up to four parameters to be determined when extracting OPE coefficients. Ultraviolet cutoff considerations, OPE convergence issues, and the need for error estimates in the fit parameters place the lattice spacing at less than 0.05 fm.

Essential information on the importance of direct instanton contributions to the OPE can be obtained from such an investigation. The OPE coefficients and vacuum expectation values are determined first by matching OPE and lattice correlation functions in which there are no direct instanton contributions. This approach determines the OPE in a self-consistent manner. Then, other correlators in which direct instanton contributions are argued to be important [31] can be examined. Discrepancies between the OPE and lattice correlation functions would signal the possible importance of direct instanton contributions. If existing predictions for direct instanton contributions to the OPE resolve the differences in the correlators, then one has compelling evidence of a non-trivial role for direct instanton contributions to the OPE. The importance of such investigations warrants further effort in this direction.

ACKNOWLEDGMENTS

The correlation functions used in this analysis were obtained in collaboration with Terry Draper and Richard Woloshyn in Ref. [1]. I wish to thank Dick Furnstahl and Xuemin Jin for a number of interesting and helpful discussions. Thanks also to Marina Nielsen for her contributions and discussions surrounding the generalized sum rules of (6.3). This research was supported by the National Science Foundation under grants No. PHY-9203145, No. PHY-9258270, No. PHY-9207889, and No. PHY-9102922.

- [1] D. B. Leinweber, R. M. Woloshyn, and T. Draper, *Phys. Rev. D* **43**, 1659 (1991).
- [2] K. Bowler *et al.*, *Nucl. Phys.* **B240**, 213 (1984).
- [3] D. B. Leinweber, this issue, *Phys. Rev. D* **51**, 6369 (1995).
- [4] Y. Chung, H. G. Dosch, M. Kremer, and D. Schall, *Nucl. Phys.* **B197**, 55 (1982).
- [5] Y. Chung, H. G. Dosch, M. Kremer, and D. Schall, *Z. Phys. C* **25**, 151 (1984).
- [6] H. G. Dosch, M. Jamin, and S. Narison, *Phys. Lett. B* **220**, 251 (1989).
- [7] B. L. Ioffe, *Nucl. Phys.* **B188**, 317 (1981).
- [8] B. L. Ioffe, *Z. Phys. C* **18**, 67 (1983).
- [9] D. B. Leinweber, *Ann. Phys. (N.Y.)* **198**, 203 (1990).
- [10] R. J. Furnstahl, D. K. Griegel, and T. D. Cohen, *Phys. Rev. C* **46**, 1507 (1992).
- [11] X. Jin *et al.*, *Phys. Rev. C* **49**, 464 (1994).
- [12] M. A. Shifman, *Vacuum Structure and QCD Sum Rules* (North-Holland, New York, 1992), p. 345.
- [13] J. Sakurai, *Advanced Quantum Mechanics* (Addison-Wesley, Reading, MA, 1967).
- [14] N. Cabibbo and E. Marinari, *Phys. Lett.* **119B**, 387 (1982).
- [15] This proved sufficient to achieve good statistical independence of the ensemble. An examination of a number of observables, configuration by configuration, revealed no apparent long-range correlation in our gauge configuration sample.
- [16] B. Efron, *SIAM Rev.* **21**, 460 (1979).
- [17] C. Michael, *Phys. Rev. D* **49**, 2616 (1994).
- [18] Particle Data Group, K. Hikasa *et al.*, *Phys. Rev. D* **45**, S1 (1992), p. III.38.
- [19] D. Richards, C. Sachrajda, and C. Scott, *Nucl. Phys.* **B286**, 683 (1987).
- [20] G. P. Lepage and P. B. Mackenzie, *Phys. Rev. D* **48**, 2250 (1993).
- [21] M. Chu, J. Grandy, S. Huang, and J. Negele, *Phys. Rev. Lett.* **70**, 255 (1993).
- [22] M. Chu, J. Grandy, S. Huang, and J. Negele, *Phys. Rev. D* **48**, 3340 (1993).
- [23] S. H. Lee, S. Choe, T. D. Cohen, and D. K. Griegel, "QCD Sum Rules and Chiral Logarithms," University of Maryland Report No. 95-067 (unpublished).
- [24] The values reported here differ from that presented in Ref. [36] due to minor differences in the renormalization procedure.
- [25] For a review of these errors and a discussion of correct sum rule analysis see Ref. [9].
- [26] S. Brodsky, J. Ellis, J. Hagelin, and C. Sachrajda, *Nucl. Phys.* **B238**, 561 (1984).
- [27] M. Gavela *et al.*, *Nucl. Phys.* **B312**, 269 (1989).
- [28] T. Schäfer, E. Shuryak, and J. Verbaarschot, *Nucl. Phys.* **B412**, 143 (1994).
- [29] M. Jamin, *Z. Phys. C* **37**, 635 (1988).
- [30] This sum rule also suffers significant uncertainty in the factorization of the dimension-6 four-quark operator.
- [31] H. Forkel and M. K. Banerjee, *Phys. Rev. Lett.* **71**, 484 (1993).
- [32] D. B. Leinweber (research in progress).
- [33] F. Wilczek, in *Lepton and Photon Interactions*, Proceedings of the 16th International Symposium, Ithaca, New York, 1993, edited by P. Drell and D. Rubin, AIP Conf. Proc. No. 302 (AIP, New York, 1994).
- [34] E. Gabrielli *et al.*, in *Lattice '90*, Proceedings of the International Symposium, Tallahassee, Florida, 1990, edited by U. M. Heller, A. D. Kennedy, and S. Sanielevici [Nucl. Phys. B (Proc. Suppl.) **20**, 448 (1991)].
- [35] P. Hasenfratz and F. Niedermayer, *Nucl. Phys.* **B414**, 785 (1994).
- [36] D. B. Leinweber, *Lattice '93*, Proceedings of the International Symposium, Dallas, Texas, edited by T. Draper *et al.* [Nucl. Phys. B (Proc. Suppl.) **34**, (1994)].
- [37] A. Thomas and B. McKellar, *Nucl. Phys.* **B227**, 206 (1983).
- [38] Y. Tomozawa, *Phys. Rev. Lett.* **46**, 463 (1981).
- [39] J. F. Donoghue and E. Golowich, *Phys. Rev. D* **26**, 3092 (1982).
- [40] M. Milosevic, D. Tadic, and J. Trampetic, *Nucl. Phys.* **B207**, 461 (1982).